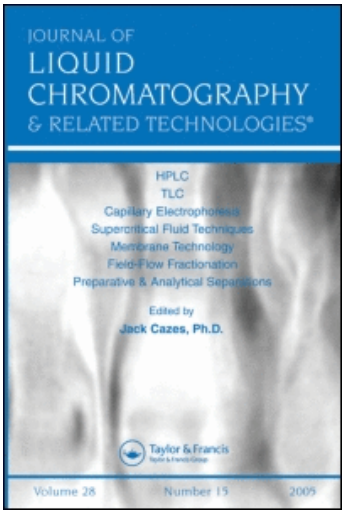

Journal of Liquid Chromatography & Related Technologies
Publication details, including instructions for authors and subscription information:
http://www.informaworld.com/smpp/title~content=t713597273

Studies on Hydrodynamic Distribution of Two Immiscible Solvent Phases in Rotating Coils

Yoichiro Ito[a]
[a] Laboratory of Technical Development, National Heart, Lung, and Blood Institute, Bethesda, Maryland

To cite this Article Ito, Yoichiro(1988) 'Studies on Hydrodynamic Distribution of Two Immiscible Solvent Phases in Rotating Coils', Journal of Liquid Chromatography & Related Technologies, 11: 1, 1 — 19
To link to this Article: DOI: 10.1080/01483919808068311
URL: http://dx.doi.org/10.1080/01483919808068311

JOURNAL OF LIQUID CHROMATOGRAPHY, 11(1), 1-19 (1988)

STUDIES ON HYDRODYNAMIC DISTRIBUTION OF TWO IMMISCIBLE SOLVENT PHASES IN ROTATING COILS

Yoichiro Ito

Laboratory of Technical Development
National Heart, Lung, and Blood Institute
9000 Rockville Pike
Bethesda, Maryland 20892

ABSTRACT

Hydrodynamic distribution of two immiscible solvent phases in rotating coils was studied with a simple rotary device. Experiments were performed with 1-2 cm I.D. glass coils, either nontreated or silicone coated, ranging in helical diameter from 2.5 to 20 cm. In general two solvent phases display characteristic four-stage distribution according to the applied rpm governed by interplay between the Archimedean screw force and radial centrifugal force. Under slow rotation the two solvent phases are evenly distributed on the head side of the coil by the Archimedean screw effect (Stage I). As the rotational speed is increased, one phase, usually the heavier phase, tends to dominate on the head side of the coil and at a critical rpm the two solvent phases are completely separated in the coil, one phase entirely occupying the head side and the other phase the tail side (Stage II). At this stage, high interfacial tension binary systems such as chloroform/water disclosed a typical effect of solvent-wall interaction in a narrow-bore coil in such a way that the aqueous phase distributed on the head side in the untreated coil whereas the nonaqueous phase occupied the head side in the silicone-coated coil. With further increase of rpm, the unilateral phase distribution declines through variety of distribution patterns (Stage III) and finally a strong radial

centrifugal force field generated by rotation establishes hydrostatic phase distribution through the coil (Stage IV). The present studies may provide valuable clues for understanding the mechanism of unilateral phase distribution in the rotating coil.

INTRODUCTION

Hydrodynamic behavior of two-phase solvent systems in a rotating coil provides an essential basis for countercurrent chromatography (CCC) [1,2]. Two immiscible solvent phases distribute themselves in a rotating coil to form various patterns of hydrodynamic equilibrium. Two phases may be distributed evenly or unilaterally along the length of the coil. The major factor which governs these hydrodynamic phenomena is the Archimedean screw force where all objects of different density are driven toward one end of the coil (this end is conventionally called the head and the other end is the tail). Other factors such as solvent-wall interaction, centrifugal force field, etc. also play important roles in hydrodynamics under certain critical conditions. Despite apparent simplicity of the system, the resultant hydrodynamics is quite complex and hardly predictable by our present knowledge.

In the past two-phase solvent distribution in the rotating coil has been extensively studied under continuous elution of mobile phase through stationary phase retained in the coil [3-8]. The report on the hydrodynamic equilibrium observed in a closed coil, however, is limited to phase distribution of chloroform/acetic acid/0.1N hydrochloric acid (2:2:1) in a 5 mm

I.D. FEP (fluorinated ethylene propylene) tube coiled in three different helical diameters [9].

The present paper describes systematic studies on hydrodynamic equilibrium in rotating glass coils of various dimensions using a set of two-phase solvent systems with a broad spectrum in hydrophobicity. Effects of solvent-wall interaction on the hydrodynamic distribution are clearly demonstrated by comparison of the phase distribution patterns obtained from each glass coil before and after silicone coating of the internal surface of the coil.

APPARATUS

A simple rotary device used in the present studies is shown in Fig. 1. It consists of a cylindrical coil holder horizontally supported between a bearing block and a motor shaft to be driven by a motor around its axis. Rotational speed is regulated from 0 to 500 rpm at high stability with a speed control unit (Bodine Electric Co., Chicago, IL). The coil holder is interchangeable to various sizes to accommodate a set of glass coils with different helical diameters.

Coils were made from glass pipes with two different internal diameters of about 1 cm and 2 cm by winding each onto brass pipes with various O.D. Size and capacity of seven glass coils are listed in Table 1. All coils are right-handed and, as shown in Table 1, I.D.'s of the large-bore coil measured along the radial dimension are considerably smaller than the nominal value of 20 mm due to flattening of the tube on winding.

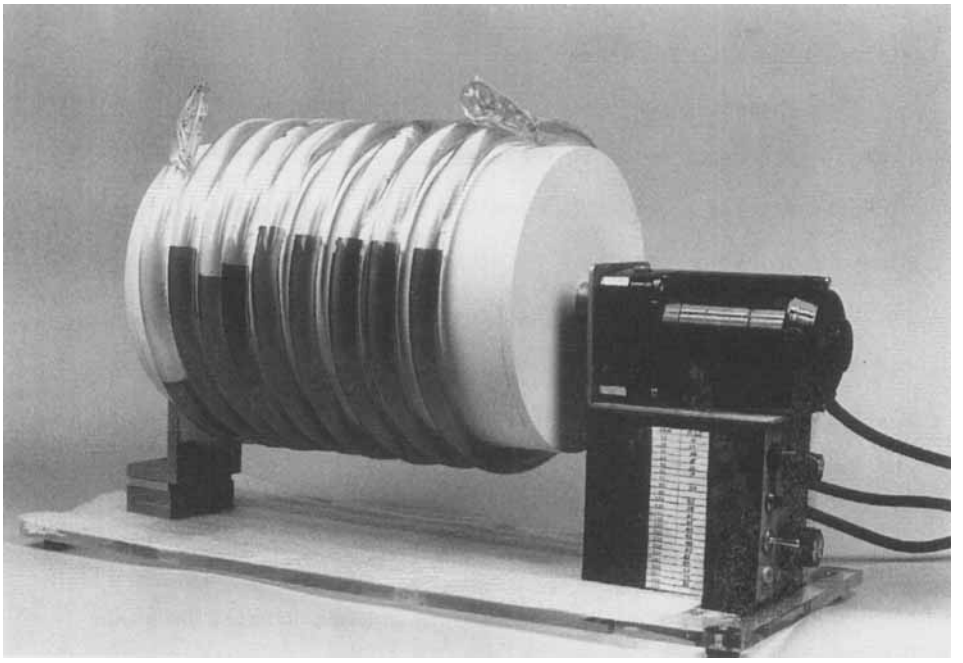

Fig. 1. Rotary coil assembly.

TABLE 1

Dimensions of Glass Coils

Core Dia. (cm)	Helical Dia. (cm)	I.D.* (mm)	O.D. (mm)	Pitch (cm)	No of Turns	Volume per Turn (ml)
2.5	3.7	9.3	11.8	1.47	13	8.6
5	6.3	9.5	12.0	1.87	12	14.6
10	11.5	10.7	13.2	1.88	10	41
20	21.7	11.6	14.1	2.20	12	70
5	7.0	17.0	19.5	3.67	9	61
10	12.1	16.5	19.0	2.67	10	93
20	22.2	16.0	18.5	2.78	9	129

* Radial

ANALYSIS OF FORCE FIELD

Centrifugal and gravitational forces acting on an arbitrary point (P) on the rotating coil with radius r is illustrated in Fig. 2. For convenience in analysis, the total force field may be expressed in two components, i.e., radially acting force, F_r, and tangentially acting force, Ft, as follows:

$$F_r = g \cos \theta + r\omega^2 = g (\cos \theta + r\omega^2/g) \quad (1)$$

$$F_t = - g \sin \theta \quad (2)$$

The sum of these forces is given by

$$F = \{(F_r)^2 + (F_t)^2\}^{1/2} = g \{1 + 2(r\omega^2/g) \cos \theta + (r\omega^2/g)^2\}^{1/2} \quad (3)$$

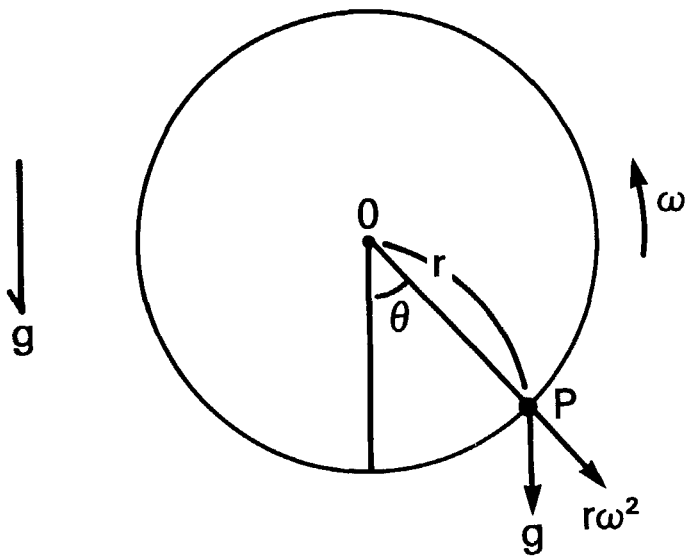

Fig. 2. Diagrams for analysis of force field acting on a rotating coil.

acting at angle

$$\gamma = \tan^{-1} \{-\sin \theta/(\cos \theta + r\omega^2)\} \quad (4)$$

Figs. 3A and B show distribution of force vectors on the rotating coils at $\omega = 5$ (A) and $\omega = 10$ (B). These diagrams indicate that the force field tends to diverge as radius r and/or angular velocity ω increases. When $r\omega^2/g = 1$, the centrifugal force created by rotation cancels the gravity at the top of the rotating coil and with further increase of the centrifugal force all vectors become radiating outwardly from the circle.

EXPERIMENTAL

Reagents

Organic solvents including n-hexane, ethyl acetate, chloroform, n-butanol, sec.-butanol, and methanol were obtained from Burdick and Jackson Laboratories, Inc., Muskegon, MI and glacial acetic acid from J. T. Baker Chemical Co.; Phillipsburg, NJ. Sudan III and acid fuchsin were purchased from Sigma Chemical Co., St. Louis, MO.

Two-Phase Solvent Systems

From the above organic solvents, following nine two-phase solvent systems were prepared: n-hexane/water, n-hexane/methanol, ethyl acetate/water, ethyl acetate/acetic acid/water (4:1:4), chloroform/water, chloroform/acetic acid/water (2:2:1), n-butanol/water, n-butanol/acetic acid/water (4:1:5), and sec.-butanol/water. Each solvent system was thoroughly

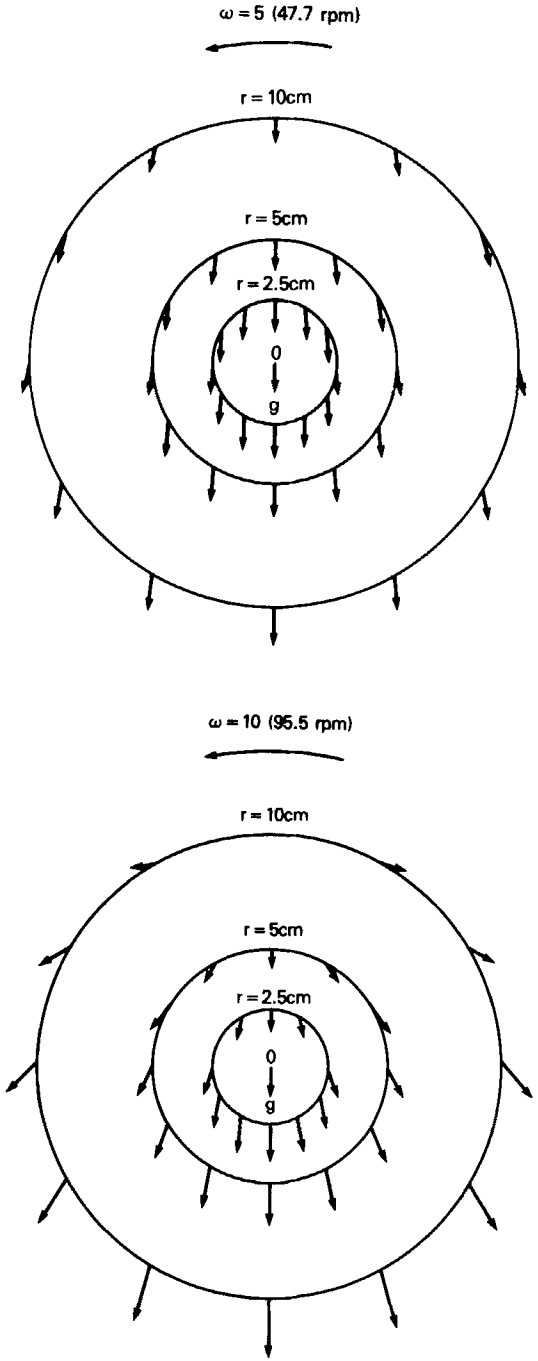

Fig. 3. Force distribution diagrams of rotating coil at 5ω (48 rpm) (A) and 10ω (96 rpm) (B).

equilibrated in a separatory funnel at room temperature. In order to facilitate observation, a small amount of sudan III was added to the nonaqueous phase of each solvent pair except that acid fuchsin was used to color the heavier phase of n-hexane/methanol which partitions Sudan III rather evenly between the two phases.

Experimental Procedure

Before experiment, the total capacity of each coil was determined by measuring the difference in weight between the empty coil and the coil filled with water. In each experiment, the coil was first filled with about equal volumes of the lighter and the heavier phases. This may be done in the following manner: one end (first terminal) of the coil is connected to a vacuum line through a fine tubing to produce gentle suction at the opposite end (second terminal) of the coil. The heavier phase measuring one half volume of the total capacity of the coil is then continuously poured into the coil through the second terminal by the aid of a funnel. After all solvent is sucked into the coil, the suction tube is disconnected from the first terminal which is then tightly closed with a glass stopper. The lighter phase is then poured into the coil through the second terminal until it nearly fills the terminal segment of the coil. After temporarily closing the second terminal with a stopper, the coil is slowly rotated in such a direction that the second terminal becomes the head. This causes movement of the air present in the coil toward the second terminal of the coil.

After one complete rotation, the stopper is removed from the second terminal to deliver more solvent into the coil. By repeating the above process, all the air present in the coil is replaced by the lighter phase. Finally, the second terminal is tightly closed with a stopper to complete the filling procedure.

Then, the coil was rotated at the lowest speed of 10 rpm. After a steady state hydrodynamic equilibrium was reached, the rotation was stopped to allow the two solvent phases to settle in each helical turn. The length of the phase segment occupying each helical turn was measured for several turns on the head side of the coil. Time required to establish the hydrodynamic equilibrium was found to vary widely ranging from a few minutes to many hours depending on the physical properties of the solvent system. Therefore, it was necessary to check phase distribution at appropriate intervals before the final measurement was made. Generally speaking, under the equilibrium condition the phase distribution becomes uniform on the head side of the coil. However, in the transitional rpm right after the unilateral distribution starts to decline, the two solvent phases occasionally form gradient volume distribution from the head toward the tail. The experiment was repeated by gradually increasing the rotational speed, until the two solvent phases established a stable hydrostatic distribution or distributed evenly throughout the coil due to a strong radial centrifugal force produced by rotation of the coil. After all solvent systems were tested with a plain glass coil, the internal wall

surface of the coil was siliconized (Siliclad obtained from Clay Adams, Parsippany, NJ) to repeat the same series of experiments to study the effect of solvent-wall interaction on the phase distribution.

Phase Distribution Diagram

The length of the phase segments measured in the above experiment does not accurately correspond to the volume of the two solvent phases present in the coil: The discrepancy becomes greater as one phase occupies more space in the helical turn. This error was corrected by directly calibrating the volume of the phase segment for each coil by injecting known amounts of lighter phase into a helical turn of the coil previously filled with the heavier phase and measuring the length of the lighter phase segment collected at the top of the coil. The set of the corrected experimental data for each measurement was averaged and the phase distribution diagram was produced by plotting percentage volume distribution of the heavier phase against the applied rotational speed in rpm for each solvent pair in each glass coil. The data obtained from the same coil, nontreated and silicone coated, are expressed in the same diagram with solid and broken curves to evaluate the effect of solvent-wall interaction.

RESULTS AND DISCUSSION

Phase Distribution Diagram

Fig. 4 shows a typical phase distribution diagram of chloroform/acetic acid/water (2:2:1) obtained from a 20 mm I.D.

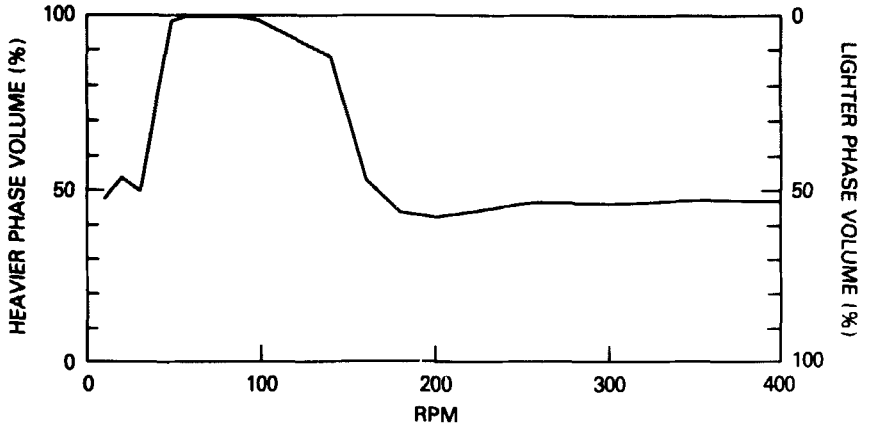

Fig. 4. Phase distribution diagrams for chloroform/acetic acid/water (2:2:1) system in 20 mm I.D. coil with 5 cm helical diameter.

untreated glass coil with 5 cm core diameter. As mentioned earlier, the ordinate indicates percentage volume distribution of the heavier phase and the abscissa, the applied rotational speed in rpm. Overall shape of the phase distribution curve is quite similar to those obtained with a 5 mm I.D. FEP (fluorinated ethylene propylene) coils previously reported and the entire curve may be divided into four stages [9].

At slow rotation of 10-20 rpm, two solvent phases are rather evenly distributed in the coil (Stage I). As the rotational speed increases, the heavier phase quickly occupies more space on the head side of the coil and at the critical speed range of 60-100 rpm, the solvent phases are completely separated along the length of the coil with the heavier phase on the head side and

the lighter phase on the tail side (Stage II). After this critical range, the amount of the heavier phase on the head side decreases sharply reaching substantially below the 50% level at 160 rpm (Stage III). Further increase of the rotational speed again distribute the two solvent phases fairly evenly throughout the coil apparently due to a strong radial centrifugal force field produced by rotation of the coil (Stage IV). The phase distribution curve of chloroform/acetic acid/water (2:2:1) described above is also followed by many other solvent systems with various minor modifications in Stages II and III.

Fig. 5 illustrates a set of phase distribution diagrams obtained from nine volatile solvent systems with a broad range in physical properties. These diagrams are arranged from left to right in the order of hydrophobicity of the major organic solvents as labelled at the top of each column whereas I.D. and core diameter of the coils are indicated on the left margin of the figure. Each diagram generally contains a pair of phase distribution curves: The solid curve was obtained from the untreated coil and the broken curve from the same coil after silicone coating. Thus, any difference between these two curves indicates the effects of solvent-wall interaction. Absence of one or both distribution curves in the designated space indicates that the two solvent phases failed to move or displayed sluggish motion in the coil and, therefore, the measurement could not be completed.

Various patterns of phase distribution curves may be conveniently described on the basis of two physical forces which

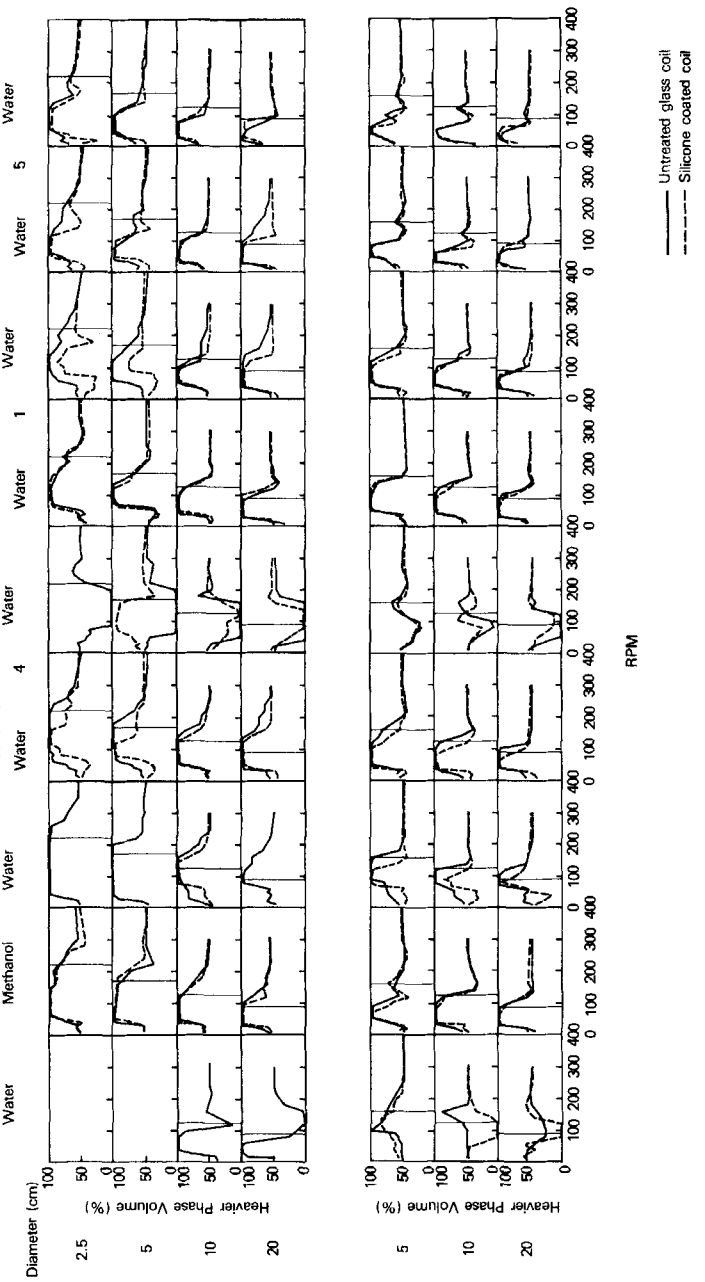

Fig. 5. Phase distribution diagrams for nine two-phase solvent systems obtained from glass coils with various dimensions (See Table 1). A thin vertical line in each diagram indicates the critical rpm where $rw^2/g = 1$.

play a major role in hydrodynamic motion of the two solvent phases in a rotating coil, i.e., solvent-wall interaction and Archimedean screw force.

1) Strong solvent-wall interaction: In the hydrophobic binary solvent systems movement of the two solvent phases through a narrow-bore coil is largely interfered by strong solvent-wall interaction. In this case segments of one phase with less wall surface affinity tends to plug the opening of the coil and the Archimedean screw force fails to break the solvent interface. Consequently, the movement of the two solvent phases in the rotating coil becomes very sluggish or completely interrupted unless application of a high rotational speed produces a strong centrifugal force field which establishes hydrostatic phase distribution in the rotating coil. Because of a strong molecular cohesive force of the aqueous phase, the above effect is enhanced in siliconized coils as observed in hexane/water and other binary solvent systems in the narrow-bore coils.

2) Combined effects: In this transitional case, two-phase flow induced by the Archimedean screw force is largely affected by solvent-wall interaction to form completely reversed modes of unilateral phase distribution between the untreated and silicone-coated coil: The aqueous phase distributes on the head side in the untreated coil while it distributes on the tail side in the siliconized coil. This peculiar phenomenon is only observed in few cases, i.e., chloroform/water in 10 mm I.D. coil with 5 cm core diameter and hexane/water in 20 mm I.D. coil with 10 cm core diameter.

3) Archimedean Screw Effect: In the rest of the cases where the solvent-wall interaction is less significant, the Archimedean screw force plays a major role in distribution of two solvent phases in the rotating coil. Under these circumstances, two solvent phases generally display characteristic distribution curve consisting of four stages as previously described for chloroform/acetic acid/water (2:2:1): even distribution at slow rotating (Stage I), unilateral distribution at the critical speed range (Stage II), reversed distribution (Stage III), and finally the hydrostatic distribution under a high rotational speed (Stage IV). As the helical diameter of the coil is increased, all these stages become proportionally shorter and shift toward the low rpm range apparently due to enhancement of the radially acting centrifugal force field.

Among these four stages, Stages I and IV are rather uniformly observed throughout all distribution curves, whereas Stages II and III display various patterns of distribution curves according to the physical properties of the solvent system. In Stage II most of the solvent systems show unilateral phase distribution with the heavier phase on the head side. Few exceptions are seen in chloroform/water and hexane/water which distribute the lighter phase toward the head side of the coil. These two solvent systems have common features of high interfacial tension associated with a large difference in density between the two phases. In addition to the above reversal of the head phase, the unilateral distribution shows a variety of shapes

in the later portion of the curve. Over the transitional zone between Stages II and III, many solvent systems display a shoulder or an indentation which gradually merges the flat 50% line at Stage IV. Hydrophilic solvent systems such as n-butanol/acetic acid/water (4:1:5) and sec.-butanol/water tend to form a minor peak which is completely isolated from the preceding major peak of Stage II. It is interesting to note that these minor peaks are observed at the critical rpm where the centrifugal force produced by rotation just cancels the gravity at the top of the rotating coil or $r\omega^2 = g$ as indicated by thin vertical lines in each diagram.

Some Speculation on the Mechanism of Unilateral Phase Distribution

Overall results of the present experiments revealed that a variety of two-phase solvent systems form unilateral phase distribution in the rotating coil. Although the mechanism involved in this hydrodynamic phenomenon is highly complex and inexplainable with our present knowledge, the present studies provide some valuable clues for speculation on this hydrodynamic mechanism.

The force distribution diagrams illustrated in Fig. 3 give interesting analogies to those produced by two different types of synchronous planetary motions shown in Fig. 6 [5]. Type I (Scheme I) synchronous planetary motion (Fig. 6, left) yields a homogeneous force distribution similar to that produced by slow coil rotation in the unit gravity (Fig. 3A) while both motions

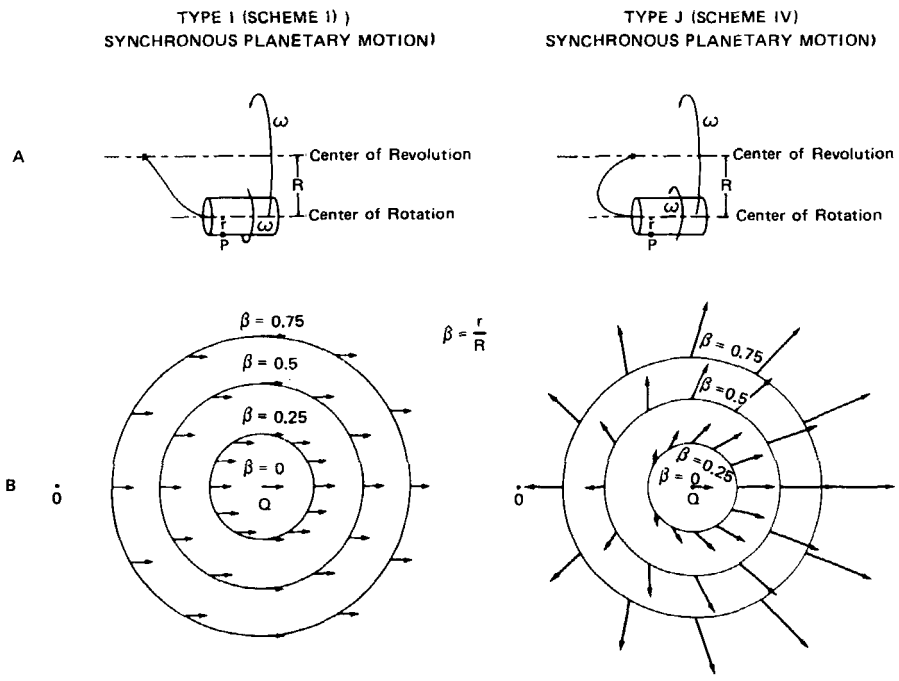

Fig. 6. Two typical modes of synchronous planetary motions (A) and their force distribution diagrams (B).

distribute two solvent phases evenly on the head side of the coil. On the other hand, Type J (Scheme IV) synchronous planetary motion (Fig. 6, right) yields a highly complex heterogeneous distribution of centrifugal force vectors which closely resembles those produced by simple coil rotation at a critical speed range (Fig. 3B). Interesting enough, these two motions establish unilateral distribution of two solvent phases in the coil. The above analogies between the simple coil rotation and two synchronous planetary motions strongly suggest that the

unilateral phase distribution may be caused by the characteristic heterogeneous force distribution which subjects the upper (or proximal) and the lower (or distal) portions of the rotating coil to uneven force fields which, in turn, provide favorable hydrodynamic condition for one of the solvent phases to move toward the head of the coil to establish a unilateral phase distribution. Under a given force field, which phase gains the favorable hydrodynamic condition may be determined by the combined effects of various factors including physical properties of the two solvent phases, solvent-wall interaction, etc.

If the above speculation proves to be the case, the sound hypothesis established on the hydrodynamics for the simple coil rotation may be further extended to the synchronous planetary motions which currently provide wide application to the advanced CCC technology.

REFERENCES

1. Ito, Y., Countercurrent Chromatography (minireview), J. Biochem. Biophys. Methods, 5(No. 2), 105, 1981.

2. Ito, Y. and Conway, W. D., Development of Countercurrent Chromatography, Anal. Chem., 56(No. 4), 534A, 1984.

3. Ito, Y. and Bowman, R. L., Preparative Countercurrent Chromatography with a Slowly Rotating Helical Tube, J. Chromatogr., 136, 189, 1977.

4. Ito, Y. A New Horizontal Flow-Through Coil Planet Centrifuge for Countercurrent Chromatography: II The Apparatus and its Partition Capabilities, J. Chromatogr., 188, 43, 1980.

5. Ito, Y., Experimental Observations of the Hydrodynamic Behavior of Solvent Systems in High-Speed Countercurrent Chromatography: Part I. Hydrodynamic Distribution of Two Solvent Phases in a Helical Column Subjected to Two Types of Synchronous Planetary Motion, J. Chromatogr., 301, 377, 1984.

6. Ito, Y., Experimental Observations of the Hydrodynamic Behavior of Solvent Systems in High-Speed Countercurrent Chromatography: Part II. Phase Distribution Diagrams for Helical and Spiral Columns, J. Chromatogr., 301, 387, 1984.

7. Ito, Y., High-Speed Countercurrent Chromatography, CRC Critical Reviews in Anal. Chem., 17(Issue 1), 65, 1986.

8. Ito, Y., A New Angle Rotor Coil Planet Centrifuge for Countercurrent Chromatography: Part II. Design of the Apparatus and Studies on Phase Distribution and Partition Capability, J. Chromatogr., 358, 325, 1986.

9. Ito, Y. and Bhatnagar, R., Improved Scheme for Preparative Countercurrent Chromatography (CCC) with a Rotating Coil Assembly, J. Liq. Chromatogr., 7(No. 2), 257, 1984.